BULLETIN OF THE EARTHQUAKE
RESEARCH INSTITUTE
Vol. 46 (1968), pp. 631-650

27. A Long Wave in the Vicinity of an Estuary [IV].

By Takao MOMOI,

Earthquake Research Institute.

(Read March 26, 1968.—Received March 30, 1968.)

Abstract

The RD (reflected and diffracted) wave around the estuary is elucidated for kd (k: the wave number of the incident wave, d: the half width of the canal) in the range 0.01 to 1.2, and the comparison of our and other authors' theories is also made.

1. Introduction

Succeeding the previous works (*Momoi*, 1965a, 1965b and 1966) on the long wave around the estuary, the behaviors of the waves reflected and diffracted around the estuary (RD waves) and the decaying waves toward the interior of the canal are elucidated numerically.

2. Simplification of the Infinite Simultaneous Equations

In the previous works, we have obtained the following infinite simultaneous equations (refer to section 2 of the first report (*Momoi*, 1965a) and section 3 of the second report (*Momoi*, 1965b)).

$$\sum_{n=0}^{\infty} I(J_{2n}, m)\cdot\bar{\zeta}_2^{(2n)} - \varepsilon_m\cdot kd\cdot\zeta_1^{(m)} = 0, \tag{1}$$

$$\sum_{n=0}^{\infty} I\left(\frac{J_{2n+1}}{r}, m\right)\cdot\zeta_2^{(2n+1)} + i\cdot\varepsilon_m\cdot k_1^{(m)}d\cdot\zeta_1^{(m)} = 0, \tag{2}$$

$$J_{2m}(kd)\cdot\bar{\zeta}_2^{(2m)} + \frac{1}{\varepsilon_m}\sum_{n=0}^{\infty}\frac{2}{\pi}\cdot\frac{(2n+1)J_{2n+1}(kd)}{(2n+1)^2-(2m)^2}\cdot\zeta_2^{(2n+1)}$$
$$= H_{2m}^{(1)}(kd)\cdot\zeta_3^{(2m)} + \frac{1}{\varepsilon_m}\cdot 2J_{2m}(kd)\cdot\zeta_0, \tag{3}$$

$$J'_{2m}(kd)\cdot\bar{\zeta}_2^{(2m)} + \frac{1}{\varepsilon_m}\sum_{n=0}^{\infty}\frac{2}{\pi}\cdot\frac{(2n+1)J'_{2n+1}(kd)}{(2n+1)^2-(2m)^2}\cdot\zeta_2^{(2n+1)}$$

$$=H_{2m}^{(1)\prime}(kd)\cdot\zeta_3^{(2m)}+\frac{1}{\varepsilon_m}\cdot 2J_{2m}'(kd)\cdot\zeta_0, \tag{4}$$

where

$$\left.\begin{aligned}&\varepsilon_0=1,\ \varepsilon_m=1/2 \qquad (m=\geq 1),\\ &I(J_{2n},\ m)=\int_0^{kd}J_{2n}(z)\cos\frac{m\pi}{kd}zdz,\\ &I\left(\frac{J_{2n+1}}{r},\ m\right)=(2n+1)\int_0^{kd}\frac{J_{2n+1}(z)}{z}\cos\frac{m\pi}{kd}zdz,\\ &k_1^{(m)}d=\sqrt{(kd)^2-(m\pi)^2},\end{aligned}\right\} \tag{5}$$

and $m=0,\ 1,\ 2,\ \text{---}$.

The model, definitions and notations employed in this paper are exactly the same as those in the previous works (*Momoi*, 1965a, 1965b and 1966), unless otherwise stated. For the model used, Fig. 1 is referred to.

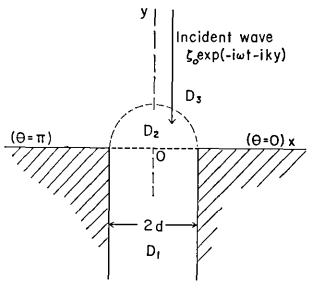

Fig. 1. Geometry of the model used.

In order to avoid the state of overflow in the electronic computer, the number of unknowns in solving simultaneous equations is diminished in the following reductions (the overflow state is caused by the existence of $\zeta_1^{(m)}$ and $\zeta_3^{(2m)}$ $(m=0,\ 1,\ 2,\ \text{---})$ in the equations for small values of kd).

Eliminating $\zeta_1^{(m)}$ from the equations (1) and (2), we have

$$i\cdot\frac{k_1^{(m)}d}{kd}\cdot\sum_{n=0}^{\infty}I(J_{2n},\ m)\bar{\zeta}_2^{(2n)}+\sum_{n=0}^{\infty}I\left(\frac{J_{2n+1}}{r},\ m\right)\zeta_2^{(2n+1)}=0 \tag{6}$$
$$(m=0,\ 1,\ 2,\ \text{---}).$$

The elimination of $\zeta_3^{(2m)}$ from (3) and (4) yields

$$\varepsilon_m\bar{\zeta}_2^{(2m)}-ikd\sum_{n=0}^{\infty}\frac{2n+1}{(2n+1)^2-(2m)^2}\cdot\{J_{2n+1}(kd)H_{2m}^{(1)\prime}(kd)-J_{2n+1}'(kd)H_{2m}^{(1)}(kd)\}\zeta_2^{(2n+1)}=2\zeta_0 \tag{7}$$
$$(m=0,\ 1,\ 2,\ \text{---}).$$

In the above reduction, the relation

$$J_{2m}(kd)H_{2m}^{(1)\prime}(kd)-J_{2m}'(kd)H_{2m}^{(1)}(kd)=2i/(\pi kd)$$

is used.

The above two equations (6) and (7) are the final forms of infinite simultaneous equations, upon which the approximation is given.

3. Fifth Approximation

In the previous paper (*Momoi*, 1966), we have already employed the theory of the fifth approximation. Then the approximated expressions of the integrations (5) have already been given in (31) and (32) of the above paper, which are rearranged in the following.

$$\left.\begin{aligned}
&I(J_0, 0)=kd-\frac{1}{12}(kd)^3+\frac{1}{320}(kd)^5,\\
&I(J_0, m)=\frac{(-1)^{m+1}}{2}\cdot\frac{1}{(m\pi)^2}(kd)^3+\frac{(-1)^m}{16}\cdot\frac{\{(m\pi)^2-6\}}{(m\pi)^4}(kd)^5 \quad (m\geq 1),\\
&I(J_2, 0)=\frac{1}{24}(kd)^3-\frac{1}{480}(kd)^5,\\
&I(J_2, m)=\frac{(-1)^m}{4}\cdot\frac{1}{(m\pi)^2}(kd)^3+\frac{(-1)^{m+1}}{24}\cdot\frac{\{(m\pi)^2-6\}}{(m\pi)^4}(kd)^5 \quad (m\geq 1),\\
&I(J_4, 0)=\frac{1}{1920}(kd)^5,\\
&I(J_4, m)=\frac{(-1)^m}{96}\cdot\frac{\{(m\pi)^2-6\}}{(m\pi)^4}(kd)^5 \qquad (m\geq 1),\\
&I(J_{2n}, m)=0 \qquad (n\geq 3,\ m\geq 0),
\end{aligned}\right\} \quad (8)$$

and

$$\left.\begin{aligned}
&I\left(\frac{J_1}{r}, 0\right)=\frac{1}{2}kd-\frac{1}{48}(kd)^3+\frac{1}{1920}(kd)^5,\\
&I\left(\frac{J_1}{r}, m\right)=\frac{(-1)^{m+1}}{8}\cdot\frac{1}{(m\pi)^2}(kd)^3+\frac{(-1)^m}{96}\cdot\frac{\{(m\pi)^2-6\}}{(m\pi)^4}(kd)^5 \quad (m\geq 1),\\
&I\left(\frac{J_3}{r}, 0\right)=\frac{1}{48}(kd)^3-\frac{1}{1280}(kd)^5,\\
&I\left(\frac{J_3}{r}, m\right)=\frac{(-1)^m}{8}\cdot\frac{1}{(m\pi)^2}(kd)^3+\frac{(-1)^{m+1}}{64}\cdot\frac{\{(m\pi)^2-6\}}{(m\pi)^4}(kd)^5 \quad (m\geq 1),\\
&I\left(\frac{J_5}{r}, 0\right)=\frac{1}{3840}(kd)^5\\
&I\left(\frac{J_5}{r}, m\right)=\frac{(-1)^m}{192}\cdot\frac{\{(m\pi)^2-6\}}{(m\pi)^4}(kd)^5 \quad (m\geq 1),\\
&I\left(\frac{J_{2n+1}}{r}, m\right)=0 \qquad (n\geq 3,\ m\geq 0).
\end{aligned}\right\} \quad (9)$$

Using (8) and (9), the equation (6) becomes

$$i\cdot\frac{k_1^{(m)}d}{kd}\cdot\sum_{n=0}^{2}I(J_{2n},\ m)\bar{\zeta}_2^{(2n)}+\sum_{n=0}^{2}I\left(\frac{J_{2n+1}}{r},\ m\right)\zeta_2^{(2n+1)}=0\quad(m=0,\ 1,\ 2),\qquad(10)$$

where the upper limit of $\sum$ is taken as 2 instead of ∞.

In the reduction of the equations (8) and (9), the Bessel function $J_m(z)$ (z: argument) is approximated by the ascending power series up to the fifth order of z. In the calculation of the Bessel function itself, the above approximated power series is not used, but the rigorous form is employed through the use of the subroutine of the Bessel function in the electronic computer. Then the Bessel function $J_m(z)$ ($m\geqq 6$) for $z\leqq kd$ is set identically equal to zero, following the fifth approximation. Using the above approximation, the equation (7) is reduced to the following.

$$\varepsilon_m\bar{\zeta}_2^{(2m)}-ikd\sum_{n=0}^{2}\frac{2n+1}{(2n+1)^2-(2m)^2}$$
$$\cdot\{J_{2n+1}(kd)H_{2m}^{(1)\prime}(kd)-J_{2n+1}'(kd)H_{2m}^{(1)}(kd)\}\zeta_2^{(2n+1)}=2\zeta_0\qquad(m=0,\ 1,\ 2),\qquad(11)$$

where the upper limit of $\sum$ is 2 instead of ∞.

Under the approximation (8), the equation (1) is reduced to

$$\zeta_1^{(m)}=\frac{1}{\varepsilon_m kd}\sum_{n=0}^{2}I(J_{2n},\ m)\bar{\zeta}_2^{(2n)}\qquad(m=0,\ 1,\ 2,\ \cdots).\qquad(12)$$

The substitution of the approximation $J_m(kd)=0$ ($m\geqq 6$) into (3) yields

$$\left.\begin{aligned}\zeta_3^{(2m)}&=\frac{1}{H_{2m}^{(1)}(kd)}\left\{J_{2m}(kd)\bar{\zeta}_2^{(2m)}-\frac{2}{\varepsilon_m}J_{2m}(kd)\zeta_0\right.\\&\left.\quad+\frac{1}{\varepsilon_m}\sum_{n=0}^{2}\frac{2}{\pi}\cdot\frac{(2n+1)J_{2n+1}(kd)}{(2n+1)^2-(2m)^2}\zeta_2^{(2n+1)}\right\}\qquad(m=0,\ 1,\ 2),\\\zeta_3^{(2m)}&=\frac{1}{iY_{2m}(kd)}\cdot\frac{4}{\pi}\sum_{n=0}^{2}\frac{(2n+1)J_{2n+1}(kd)}{(2n+1)^2-(2m)^2}\zeta_2^{(2n+1)}\quad(m=3,\ 4,\ 5,\cdots).\end{aligned}\right\}\qquad(13)$$

Solving the equations (10) and (11) with the help of the electronic computer, the unknown factors

$$\bar{\zeta}_2^{(2m)}\quad\text{and}\quad\zeta_2^{(2m+1)}\quad(m=0,\ 1,\ 2)\qquad(14)$$

in the domain D_2 are obtained.

Substituting the above known factors into (12) and (13), the factors

$$\zeta_1^{(m)}\quad\text{and}\quad\zeta_3^{(2m)}\quad(m=0,\ 1,\ 2,\cdots)\qquad(15)$$

respectively in the domains D_1 and D_3 begin to be known.

Under the fifth approximation, the formal expressions of the wave are:

$$\zeta_1=\sum_{m=0}^{\infty}\zeta_1^{(m)}\cos\frac{m\pi}{d}x\cdot e^{-ik_1^{(m)}y} \tag{16}$$

in the domain D_1,

$$\zeta_2=\sum_{n=0}^{2}\{\zeta_2^{(2n)}\cos 2n\theta J_{2n}(kr)+\zeta_2^{(2n+1)}\sin(2n+1)\theta J_{2n+1}(kr)\} \tag{17}$$

in the domain D_2,

$$\zeta_3=2\zeta_0\cos ky+\sum_{n=0}^{\infty}\zeta_3^{(2n)}\cos 2n\theta H_{2n}^{(1)}(kr) \tag{18}$$

in the domain D_3,

where, for the derivation of the first and third expressions, reference should be made to the previous paper (*Momoi*, 1965a) and, for the second expression, the reader should refer to the paper (*Momoi*, 1965a) and (39) of the paper (*Momoi*, 1966).

Using the factors obtained in (14) to (15), the behaviors of the wave around the estuary are elucidated through the expressions (16) to (18).

In the numerical calculation by use of the previous theory of the fifth approximation (refer to section 6 of the paper (*Momoi*, 1966)), the state of overflow in the computer took place for the value less than $kd\fallingdotseq 0.5$ so that the numerical calculation in the range $kd\leqq 0.5$ resorts to the theory of less order of approximation. In order to avoid this difficulty, the improvement of the theory has been carried out in the present paper. According to the result of the numerical calculation, the theory of the present paper makes possible the calculation up to $kd=0.01$ at least.

4. Sixth Approximation

In this section, the theory of the sixth approximation is developed.

In the reduction of the integration (5), the Bessel function $J_m(z)$ is retained up to the sixth order of z of the ascending power series. Under this approximation, the integration (5) becomes:

$$
\left.
\begin{aligned}
I(J_0, 0) &= \{I(J_0, 0) \text{ of 5th appr.}\} - \frac{1}{(2\cdot4\cdot6)^2}\cdot\frac{1}{7}(kd)^7, \\
I(J_0, m) &= \{I(J_0, m) \text{ of 5th appr.}\} \\
&\quad + \frac{(-1)^{m+1}}{(2\cdot4\cdot6)^2}\cdot\frac{\{6(m\pi)^4-120(m\pi)^2+720\}}{(m\pi)^6}(kd)^7 \quad (m\geq1), \\
I(J_2, 0) &= \{I(J_2, 0) \text{ of 5th appr.}\} + \frac{1}{2!\cdot4!\cdot2^6}\cdot\frac{1}{7}(kd)^7, \\
I(J_2, m) &= \{I(J_2, m) \text{ of 5th appr.}\} \\
&\quad + \frac{(-1)^{m}}{2!\cdot4!\cdot2^6}\cdot\frac{\{6(m\pi)^4-120(m\pi)^2+720\}}{(m\pi)^6}(kd)^7 \quad (m\geq1), \\
I(J_4, 0) &= \{I(J_4, 0) \text{ of 5th appr.}\} - \frac{1}{5!\cdot2^6}\cdot\frac{1}{7}(kd)^7, \\
I(J_4, m) &= \{I(J_4, m) \text{ of 5th appr.}\} \\
&\quad + \frac{(-1)^{m+1}}{5!\cdot2^6}\cdot\frac{\{6(m\pi)^4-120(m\pi)^2+720\}}{(m\pi)^6}(kd)^7 \quad (m\geq1), \\
I(J_6, 0) &= \frac{1}{6!\cdot2^6}\cdot\frac{1}{7}(kd)^7, \\
I(J_6, m) &= \frac{(-1)^{m}}{6!\cdot2^6}\cdot\frac{\{6(m\pi)^4-120(m\pi)^2+720\}}{(m\pi)^6}(kd)^7 \quad (m\geq1), \\
I(J_{2n}, m) &\quad (n\geq4,\ m\geq0),
\end{aligned}
\right\} \tag{19}
$$

and

$$
\left.
\begin{aligned}
&I\left(\frac{J_{2n+1}}{r}, m\right) \quad (n\geq0,\ m\geq0) \text{ having identically the same} \\
&\text{expressions as those given in the fifth approximation} \\
&\text{(refer to (9)).}
\end{aligned}
\right\} \tag{20}
$$

Under the approximations (19) and (20), the infinite number of equations (6) is reduced to the finite number of equations as follows.

$$
i\cdot\frac{k_1^{(m)}d}{kd}\cdot\sum_{n=0}^{3} I(J_{2n}, m)\bar{\zeta}_2^{(2n)} + \sum_{n=0}^{2} I\left(\frac{J_{2n+1}}{r}, m\right)\zeta_2^{(2n+1)} = 0 \quad (m=0,\ 1,\ 2), \tag{21}
$$

where the upper limits of the first and second $\sum$ are 3 and 2 respectively.

In the same way as in the case of the fifth approximation, the calculation of the Bessel function $J_m(z)$ itself is not made by the approximated power series (taken up to the six orders of z), but the

rigorous calculation is made by use of the subroutine of the above function, being retained $J_m(z)$ $(m \leqq 6)$ only (others are set identically equal to zero).

Retaining the Bessel function $J_m(kd)$ up to $m=6$, the equation (7) becomes

$$\varepsilon_m \overline{\zeta}_2^{(2m)} - ikd \sum_{n=0}^{2} \frac{2n+1}{(2n+1)^2-(2m)^2} \cdot \{J_{2n+1}(kd) H_{2m}^{(1)\prime}(kd) - J'_{2n+1}(kd) H_{2m}^{(1)}(kd)\} \zeta_2^{(2n+1)} = 2\zeta_0 \quad (m=0, 1, 2, 3), \tag{22}$$

where m is taken up to 3 instead of 2, though the form of the above equation is exactly the same as that in (11) for the case of the fifth approximation.

Under the assumption (19), the equation (1) becomes

$$\zeta_1^{(m)} = \frac{1}{\varepsilon_m kd} \sum_{n=0}^{3} I(J_{2n}, m) \overline{\zeta}_2^{(2n)} \quad (m=0, 1, 2, \cdots). \tag{23}$$

In the above expression, the upper limit of $\sum$ is taken 3.

Using the approximation $J_m(kd) \equiv 0$ for $m \geqq 7$ corresponding to the sixth approximation, the expression for obtaining the factor $\zeta_3^{(2m)}$ in the domain D_3 becomes, from (3), as follows.

$$\left.\begin{aligned} &\zeta_3^{(2m)} = \{\text{the r.h.s. of the 1st equation of (13)}\} \\ &\qquad (m=0, 1, 2, 3,) \\ \text{and} \\ &\zeta_3^{(2m)} = \{\text{the r.h.s. of the 2nd equation of (13)}\} \\ &\qquad (m=4, 5, 6, \cdots), \end{aligned}\right\} \tag{24}$$

where r.h.s. stands for right-hand side. In (24), the first equation is taken up to $m=3$ instead of 2 in (13), so that the second one begins with $m=4$ instead of 3 in (13).

Solving (21) and (22), the unknown factors

$$\overline{\zeta}_2^{(2m)} \quad \text{and} \quad \zeta_2^{(2n+1)} \quad (m=0, 1, 2, 3;\ n=0, 1, 2) \tag{25}$$

are obtained.

The substitution of the above factors into (23) and (24) makes possible the calculations of the factors.

$$\zeta_1^{(m)} \quad \text{and} \quad \zeta_3^{(2m)} \quad (m=0, 1, 2, \cdots). \tag{26}$$

Under the sixth approximation, the formal expression of the wave in the domain D_2 becomes

$$\zeta_2=\sum_{n=0}^{3}\bar{\zeta}_2^{(2n)}\cos 2n\theta J_{2n}(kr)+\sum_{n=0}^{2}\zeta_2^{(2n+1)}\sin(2n+1)\theta J_{2n+1}(kr), \qquad (27)$$

retaining the $J_m(kr)$-terms up to $m=6$ in (8) of the paper (*Momoi*, 1965a).

As far as the formal expressions in the domains D_1 and D_3 are concerned, the forms are exactly the same as those in (16) and (18).

Now, in the same way as that in the case of the fifth approximation, the waves around the estuary are elucidated through the substitution of (25) and (26) into (16), (18) and (27).

5. RD wave

When the incident wave arrives at the coast, the wave is reflected and diffracted subjecting to the configuration of the coast. The wave reflected and diffracted (RD wave) is expressed by the forms:

$$\zeta_{rd}^{(j)}=\zeta_j-\zeta_0 e^{-iky} \qquad (j=1,\ 2,\ 3), \qquad (28)$$

where $\zeta_{rd}^{(j)}$ $(j=1,\ 2,\ 3,)$ is the height of the RD wave respectively in the domains D_j $(j=1,\ 2,\ 3)$, ζ_j $(j=1,\ 2,\ 3)$ being the resultant wave (RST wave) given by (16), (17) (or (27)) and (18). As shown in (28), the RD wave is a purely reflected and diffracted wave excluding the incident wave.

The calculated results in the cases of $kd=0.01$ to 1.2 are shown in Figs. 2a to 13a for the amplitude and in Figs. 2b to 13b for the phase. The amplitude is calculated by $|\zeta_{rd}^{(j)}|$ $(j=1,\ 2,\ 3)$ which is normalized by the amplitude of the incident wave and the phase by $\arg\zeta_{rd}^{(j)}$ $(j=1,\ 2,\ 3)$. The calculations are based on the theory of the fifth approximation.

To begin with, the variation of the amplitude is discussed. Inspection of the figures concerning the amplitude variation (Figs. 2a to 13a) reveals that a portion of high wave extends to the interior of the canal with decaying sense (see Fig. 14). When the wave-length is very long (the cases of Figs. 2a, 3a and 4a), the wave diffracted toward the canal is nearly equal to 1.0 in amplitude. As kd increases, the amplitude of the above wave decreases monotonically to zero (see Figs. 5a to 13a). In the open sea, a minimum wave height appears at a point slightly

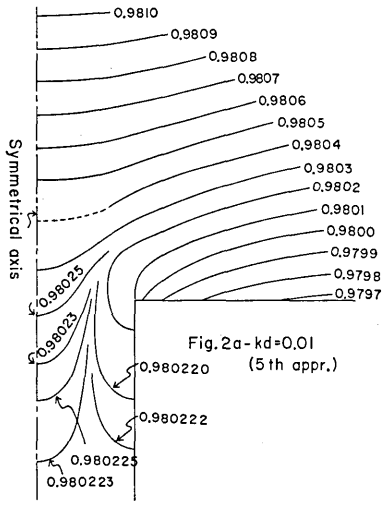

Fig. 2a. Variation of the amplitude of RD wave for $kd=0.01$. The values stated in the figure denote the amplitude of RD wave which is normalized by the amplitude of the incident wave. The following eleven figures are depicted in the same way.

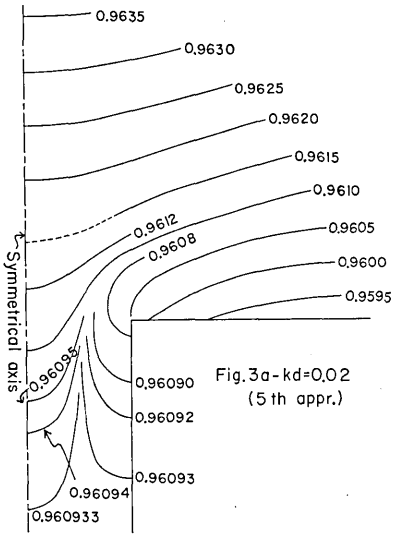

Fig. 3a. Variation of the amplitude of RD wave for $kd=0.02$.

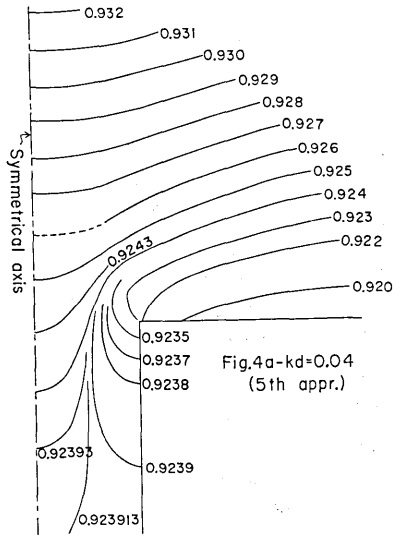

Fig. 4a. Variation of the amplitude of RD wave for $kd=0.04$.

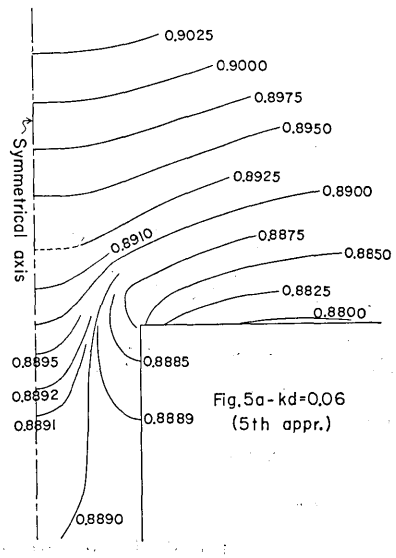

Fig. 5a. Variation of the amplitude of RD wave for $kd=0.06$.

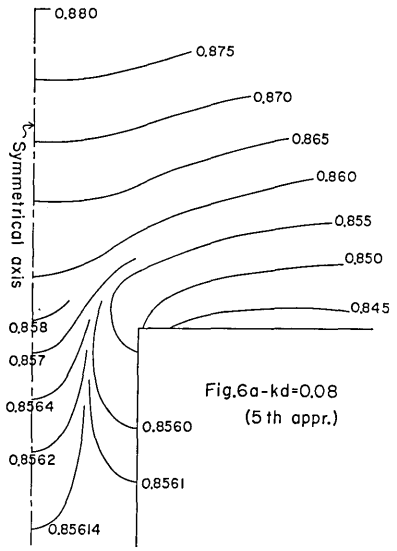

Fig. 6a. Variation of the amplitude of RD wave for $kd=0.08$.

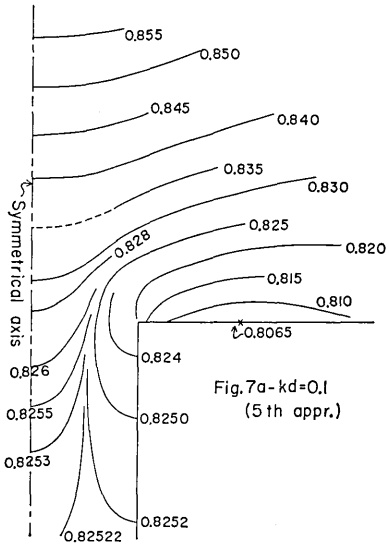

Fig. 7a. Variation of the amplitude of RD wave for $kd=0.1$.

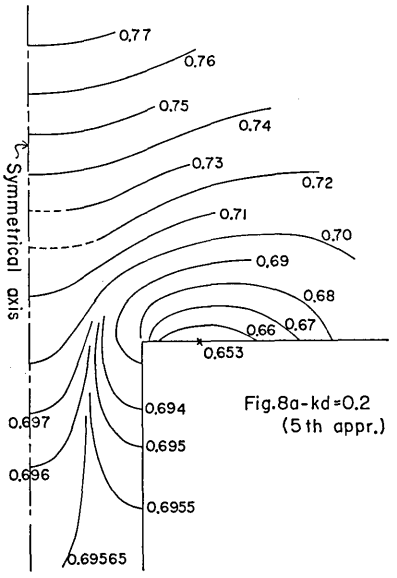

Fig. 8a. Variation of the amplitude of RD wave for $kd=0.2$.

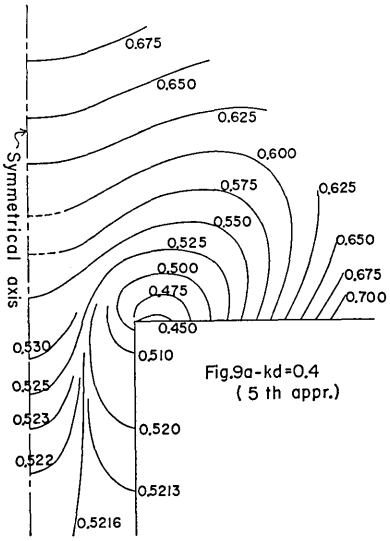

Fig. 9a. Variation of the amplitude of RD wave for $kd=0.4$.

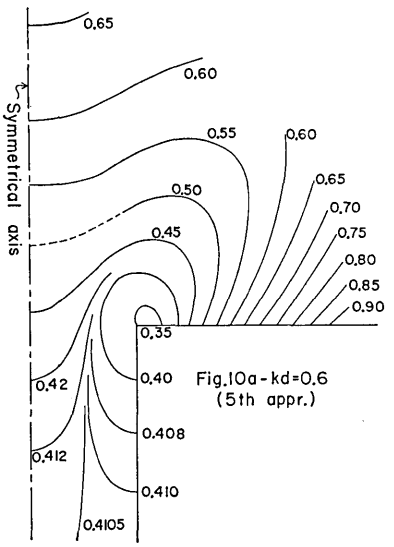

Fig. 10a. Variation of the amplitude of RD wave for $kd=0.6$.

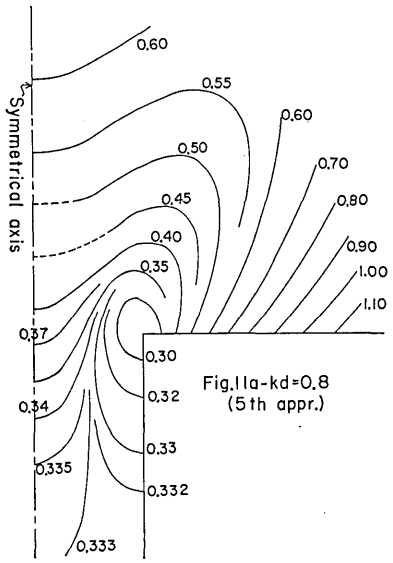

Fig. 11a. Variation of the amplitude of RD wave for $kd=0.8$.

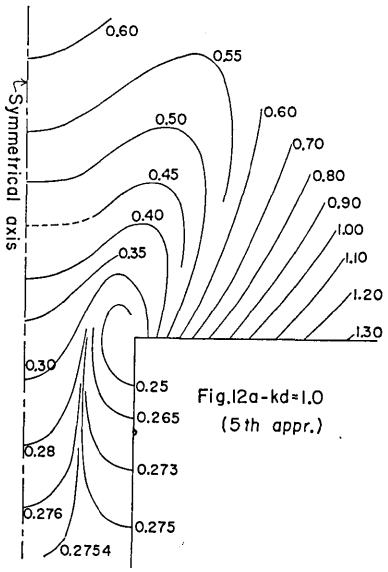

Fig. 12a. Variation of the amplitude of RD wave for $kd=1.0$.

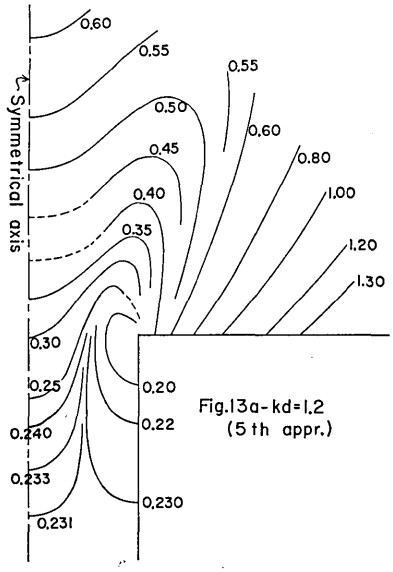

Fig. 13a. Variation of the amplitude of RD wave for $kd=1.2$.

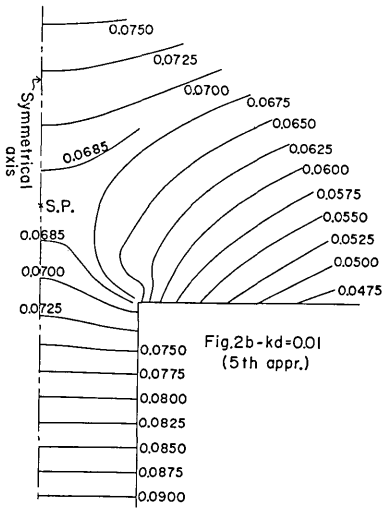

Fig. 2b. Variation of the phase of RD wave for $kd=0.01$. The values stated in the figure denote $\arg \zeta_{rd}^{(j)}$ $(j=1, 2, 3)$, the letters S. P. being the abbreviation of the stagnation point. Under the same convention, the following eleven figures are depicted.

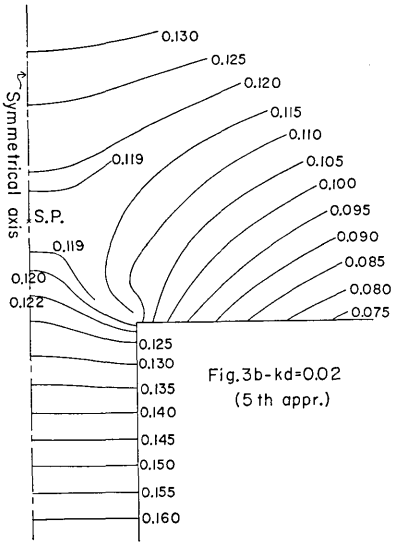

Fig. 3b. Variation of the phase of RD wave for $kd=0.02$.

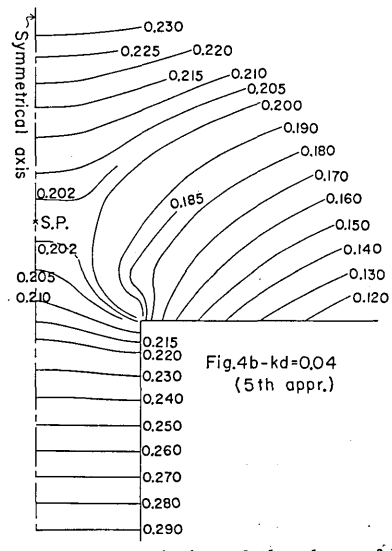

Fig. 4b. Variation of the phase of RD wave for $kd=0.04$.

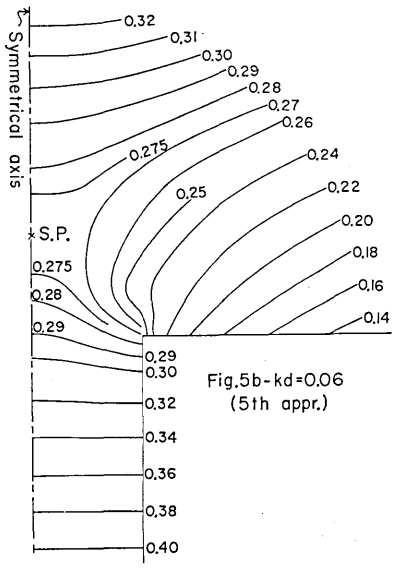

Fig. 5b. Variation of the phase of RD wave for $kd=0.06$.

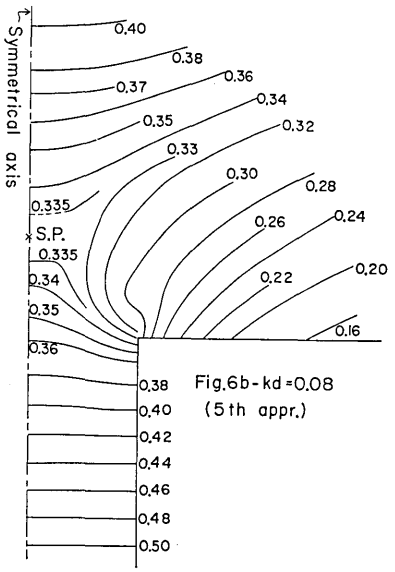

Fig. 6b. Variation of the phase of RD wave for $kd=0.08$.

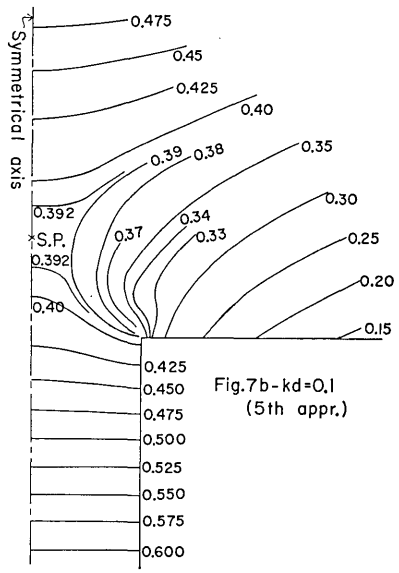

Fig. 7b. Variation of the phase of RD wave for $kd=0.1$.

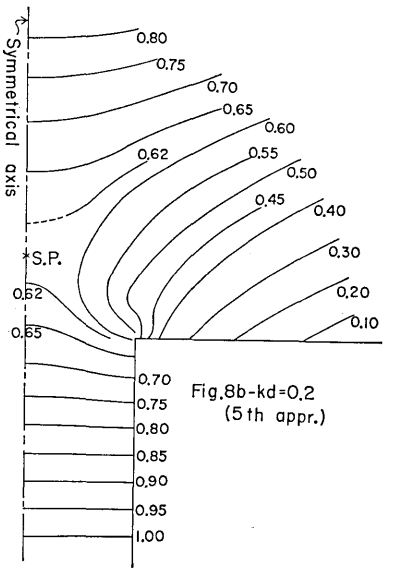

Fig. 8b. Variation of the phase of RD wave for $kd=0.2$.

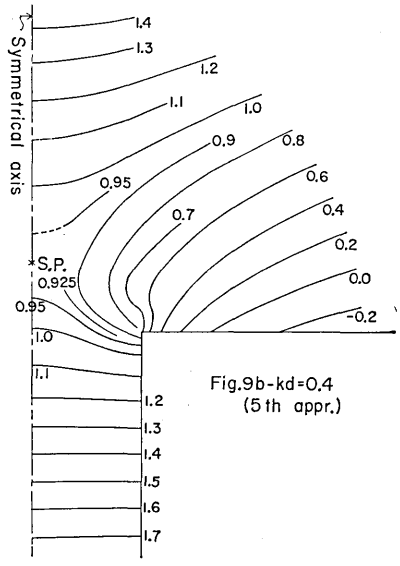

Fig. 9b. Variation of the phase of RD wave for $kd=0.4$.

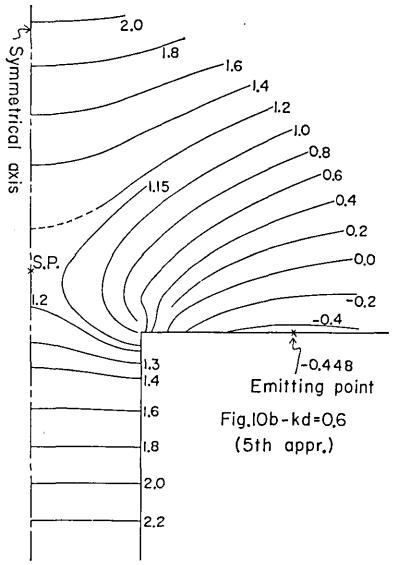

Fig. 10b. Variation of the phase of RD wave for $kd=0.6$.

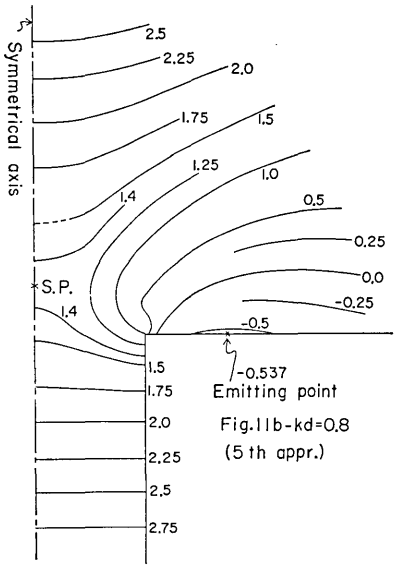

Fig. 11b. Variation of the phase of RD wave for $kd=0.8$.

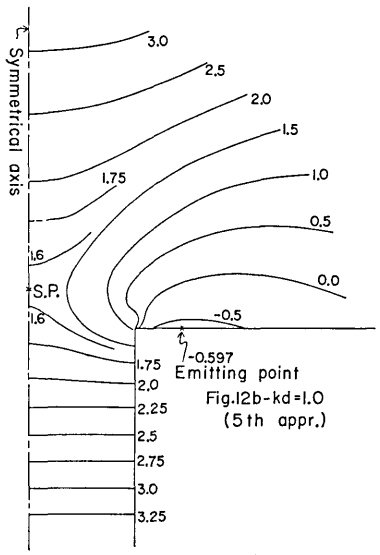

Fig. 12b. Variation of the phase of RD wave for $kd=1.0$.

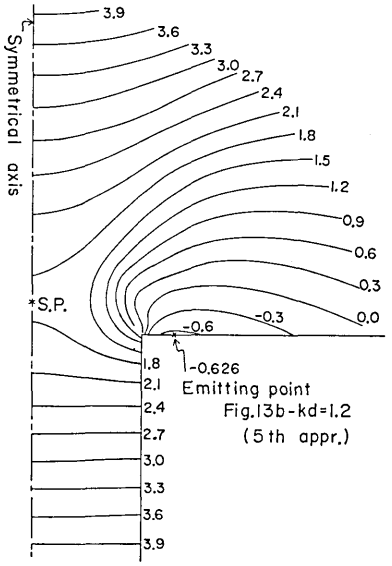

Fig. 13b. Variation of the phase of RD wave for $kd=1.2$.

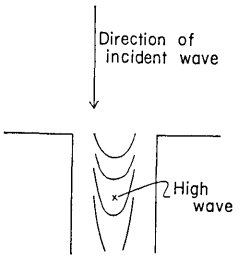

Fig. 14. Generation of the high wave in the interior of the canal.

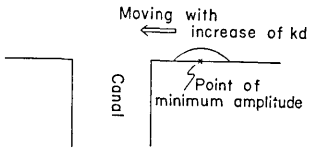

Fig. 15. Behavior of a point of minimum amplitude at the coast.

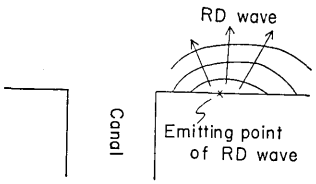

Fig. 16. Emission of RD wave from the coast near the estuary.

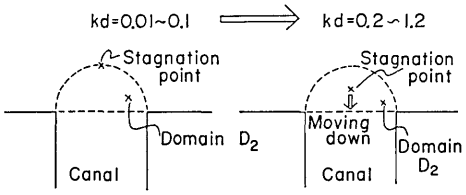

Fig. 17. Behavior of the stagnation point of RD wave for the variation of *kd*.

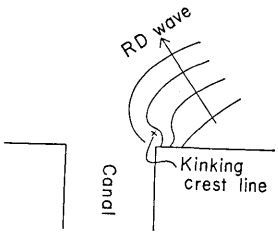

Fig. 18. Appearance of the kinking crest line in the waters near the corner of the estuary.

away from the corner of the estuary along the coast. The above minimum point gradually approaches the corner with increase of *kd* (see Fig. 15). When $kd \fallingdotseq 1.0$, the minimum point reaches the leading part of the canal.

Next, mention is made of the variation of phase which is depicted in Figs. 2b to 13b. Passing through the above figures, it is found that the RD wave emits from the point slightly away from the mouth of the canal along the coast facing the open sea (see Fig. 16). The emitting point moves to the corner of the estuary as *kd* increases. The above emitted waves are propagated partly toward the open sea and partly toward the mouth of the canal, causing the stagnating point of the wave (this point is stated by S. P. in Figs. 2b to 13b). When *kd* is small, say the cases of Figs. 2b to 7b, the stagnation point is located at the outer margin of the domain D_2 (see Fig. 17). When *kd* increases, the above stagnation point moves down toward the canal (refer to Figs. 8b to 13b). The above tendency of the stagnation point is in accordance with the triangularity of the crest line for small *kd* and the flattening nature of the trapezoid of the crest line with increase of *kd* (refer to

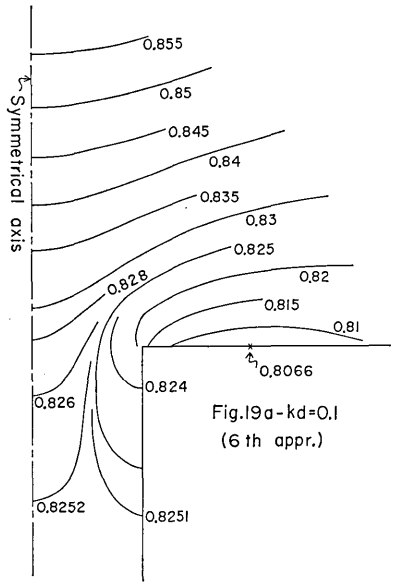

Fig. 19a. Variation of the amplitude of RD wave for $kd=0.1$. The values stated in the figure denote the amplitude of RD wave (normalized by the amplitude of the incident wave) which is calculated by use of the theory of the sixth approximation. In Fig. 20a, the calculation was made in the same way.

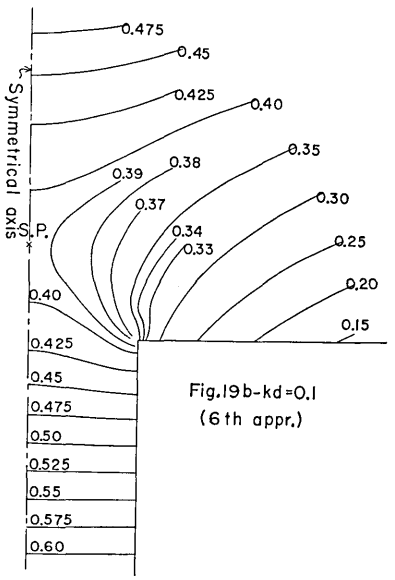

Fig. 19b. Variation of the phase of RD wave for $kd=0.1$. The values stated in the figure denote $\arg \zeta_{rd}^{(j)}$ $(j=1, 2, 3)$ which is calculated by use of the theory of the sixth approximation. In Fig. 20b, the calculation was made in the same way.

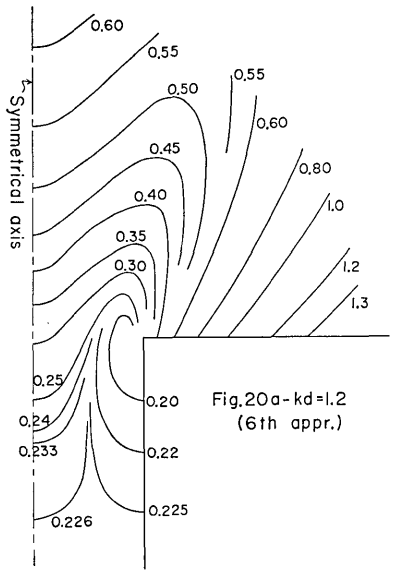

Fig. 20a. Variation of the amplitude of RD wave for $kd=1.2$.

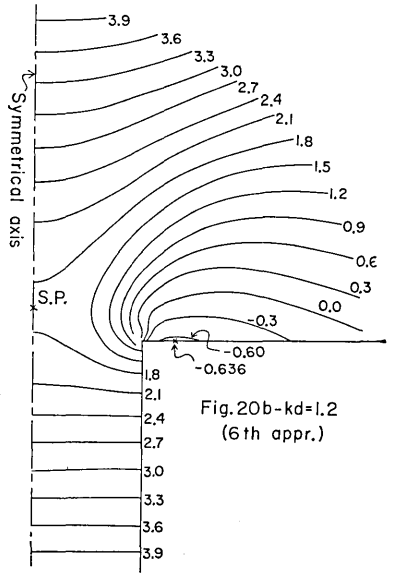

Fig. 20b. Variation of the phase of RD wave for $kd=1.2$.

Fig. 9 of the paper (*Momoi*, 1966)). Through the figures relevant to the phase variation of the RD wave, another conspicuous feature is an appearance of the kinking crest line in the waters near the corner of the estuary (see Fig. 18). In the work concerning the long wave around the breakwater (*Momoi*, 1967), the kinking nature of the phase line near the terminus of the breakwater wing is not found in the figure relevant to the RD wave (refer to Fig. 23(p) of the above paper). The generation mechanism of the above kinking phase line of the RD wave near the corner of the estuary seems to be the result of the scattering of the wave after the collision of the wave diffracted from the corner (left-hand one in Fig. 1) to the wall of the canal near the other corner (righthand one in Fig. 1). Concerning this problem, further verification will be made in the subsequent work.

In order to avoid the misunderstanding that the above results of the RD wave might arise from the approximation used, the figures based on the theory of the sixth approximation are prepared in Figs. 19a (19b) and 20a (20b) for the amplitude (phase) variation of $kd=0.1$ and 1.2. According to these figures, the above-mentioned results are found to be the established facts that do not come from the employed approximation.

6. Comparison with Other Theories

When the width of the canal is narrow, the approximated theory is developed by Mitsui (*Mitsui*, 1966). In his theory, the wave invading the canal is assumed as a uniform advancing wave which does not include the decaying (higher) modes. Using the Fourier-transform technique, he obtained the amplitude variations of the advancing wave to the canal and of the wave along the coast facing the open sea. His numerical results are reproduced in Figs. 21 to 23 (his curves are denoted by Mitsui's curve in the figures). Inspection of Fig. 21 (in which the amplitude of the advancing wave in the canal is shown) reveals a very good agreement of Mitsui's and Momoi's curves. This result shows that our discussion of the advancing wave of the canal (not including the higher modes) might be possible up to the range of $kd=1.0$ at least. In Figs. 22 and 23, the amplitudes of the wave along the straight coast are depicted for $kd=0.52465$ ($2d/L=0.167$, L: the wave-length of the incident wave) and 1.0 ($2d/L=0.318$) comparing with Mitsui's results. The extent of agreement of the two author's curves is fairly good with a slight difference in that the agreement in Fig. 22 (the case of $kd=0.52465$) is

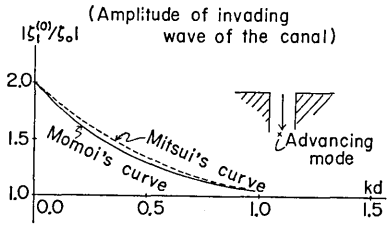

Fig. 21. Comparison of Mitsui's and Momoi's results of the amplitude of the advancing wave in the canal.

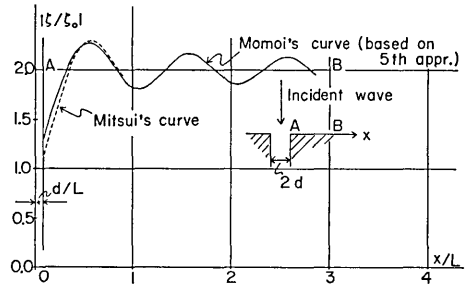

Fig. 22. Comparison of Mitsui's and Momoi's results of the amplitude of the wave along the coast for $kd=0.52465$.

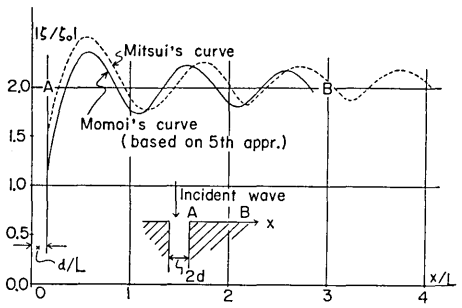

Fig. 23. Comparison of Mitsui's and Momoi's results of the amplitude of the wave along the coast for $kd=1.0$.

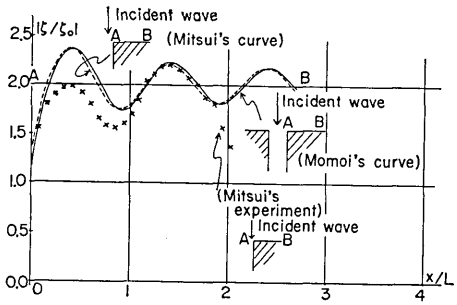

Fig. 24. Comparison of Mitsui's result (the amplitude variation of the wave along the coast facing the incident wave in the model of the right-angled corner) and Momoi's (the amplitude variation along the coast of the estuary for $kd=1.0$).

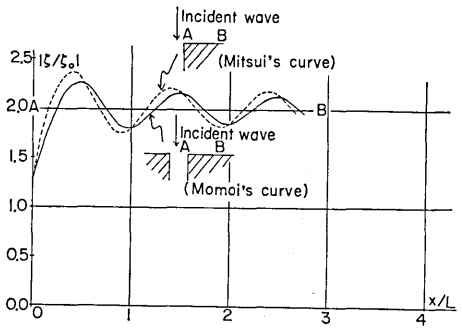

Fig. 25. Comparison of Mitsui's (the same variation as that in Fig. 24) and Momoi's (the amplitude variation along the coast of the estuary for $kd=0.52465$).

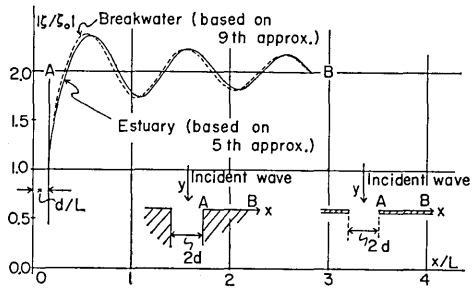

Fig. 26. Comparison of the amplitude variations of the wave along the coast of the estuary and along the windward part of the breakwater for $kd=1.0$.

rather better than that in Fig. 23 (the case of $kd=1.0$). The better agreement of the former is interpreted as being due to the approximation used in Mitsui's work.

Mitsui also calculated the amplitude of the wave along the coast which has a right-angled corner, making the experiment for the same model (refer to Fig. 12(b) of Mitsui's paper (*Mitsui*, 1967)). Mitsui's results are reproduced in Figs. 24 and 25, in which his computed curve is denoted by Mitsui's curve and in the former of which the experimental data made by Mitsui is also arranged. In the above two figures, the amplitude variation of the coast in the estuary is also presented. Inspection of the figures shows that the variations of the amplitude of two different models (one is the right-angled corner and the other the canal) are so alike that the waves along the coast normal to the direction of the incident wave travel in two models might be considered as behaving in a similar way. The resemblance of the curves is greater in Fig. 24 (the case of $kd=1.0$) than in Fig. 25 (the case of $kd=0.52465$). This result is due to the fact that the coupling effect of the two corners of the estuary is greater for small kd than for large kd. When $kd=1.0$ (the case of Fig. 24), the coupling of the two coasts of the estuary is almost not found. This fact implies that the method of the mirror image of the single right-angled corner might be useful for the analysis of the wave around the estuary in the range $kd>1.0$.

In Fig. 26, the comparison of the amplitudes of the RST wave along the coast of the estuary and along the windward part of the breakwater is made for the parameter $kd=1.0$. Conspicuous agreement of the two curves is found in the figure. This agreement suggests a quite similar behavior of the wave in the waters, exposed to the incident wave, of the above two models when $kd=1.0$.

References

MITSUI, H., 1966, Distribution of Wave Height in the nearby Region of the Discontinuous Part of Coastal Structures (the first report) (in Japanese), *Collected Papers of the Thirteenth Coastal Engineering Conference*, 80-86.

MITSUI, H., 1967, Distribution of Wave Height in the nearby Reigion of the Discontinuous Part of Coastal Structures (the second report) (in Japanese), *Collected Papers of the Fourteenth Coastal Engineering Conference*, 53-59.

MOMOI, T., 1965a, A Long Wave in the Vicinity of an Estuary [I], *Bull. Earthq. Res. Inst.*, **43**, 291-316.

MOMOI, T., 1965b, A Long Wave in the Vicinity of an Estuary [II], *Bull. Earthq.*

Res. Inst., **43**, 459-498.

MOMOI, T., 1966, A Long Wave in the Vicinity of an Estuary [III], *Bull. Earthq. Res. Inst.*, **44**, 1009-1040.

MOMOI, T., 1967, A Long Wave around a Breakwater [II], *Bull. Earthq. Res., Inst.*, **45**, 749-783.

---

27. 河口近傍における長波について [IV]

地震研究所　桃　井　高　夫

本報告においては河口近傍での RD (反射回折) 波について，kd (k: 入射波の波数，d: 水路の巾の半分の長さ) が 0.01 より 1.2 までの範囲について論じられている．又筆者の理論と他の理論との比較がなされている．
